ADVANCED FUNCTIONAL MATERIALS
www.afm-journal.de

Tetradentate Platinum Complexes for Efficient and Stable Excimer-Based White OLEDs

*Tyler Fleetham, Liang Huang, and Jian Li**

A series of tetradentate platinum complexes that exhibit both efficient monomer and excimer emission are synthesized. Via small modifications to the cyclometalating ligands, both the monomer and excimer emission energy can be separately tuned. Devices employing all of the developed emitters demonstrate impressively high external quantum efficiencies (EQEs) within the range of 22% to 27% for concentrations between 2% and 16%. The halogen-free design of the complexes also enables the fabrication of single, doped, white organic light-emitting diodes (OLEDs) with long operational lifetimes. A balanced white device employing the complex Pt2O2, achieves a device operational lifetime to 80% of the initial luminance estimated at over 200 h at 1000 cd m^{-2}, while also achieving 12.5% peak EQE for a warm white light with a color rendering index of 80. Furthermore, a highly doped device exhibiting nearly exclusive excimer emission showed an impressive operational lifetime, which is estimated at more than 400 h for 1000 cd m^{-2}.

1. Introduction

Organic light-emitting devices (OLEDs) have been widely studied as potential next generation energy efficient displays and solid state lighting for their benefits of potentially low fabrication cost, high energy efficiency, and the ability to be fabricated in a number of different form factors on various substrates.[1] Through diligent materials design and the continual development of new device architectures, red, green, and blue OLEDs with high quantum efficiency and desirable color coordinates have been developed.[2–4] In particular, the incorporation of phosphorescent Ir and Pt complexes have yielded very high device efficiencies across the visible spectrum due to their ability to harvest 100% of electrogenerated excitons.[5,6] There has also been much progress on the development of materials and device structures for white OLEDs (WOLEDs) for lighting applications.[7] The potential for high power efficiency and potentially low fabrication cost makes WOLEDs highly desirable candidates to replace inefficient incandescent or fluorescent bulbs and compete with expensive inorganic lighting technologies.[8] Most of the best reported WOLEDs have employed multiple emissive materials either as a single layer with multiple emissive dopants, in multiple emissive layers, or through the combination of fluorescent and phosphorescent materials.[9–11] With these structures, typically employing iridium complexes, WOLEDs have achieved external quantum efficiencies over 20%, color rendering index (CRI) over 80, and power efficiencies over 100 lm/W when advanced outcoupling techniques are employing.[12] However, the strategy of using multiple emissive materials depends on the precise control over various energy transfer processes within the device which can significantly complicate the device fabrication and have significant tradeoffs between device efficiency and emission color.[13] Furthermore, the precise color balance of WOLEDs containing multiple emissive materials can be significantly perturbed by variations in the driving conditions, or through different aging processing of the various materials.[14] Thus, it is strongly desired to achieve an efficient WOLED containing a single emissive material which is efficient, stable, and can be fabricated within a single emissive layer.

One major approach to achieve single doped white OLEDs is through the exploitation of the excimer emission properties of square planar complexes for a broad white emission.[15] In excimer based OLEDs, white emission is achieved through the combination of blue emission from an isolated dopant molecule and orange-red emission of two or more closely stacked dopant molecules. Much of the existing reports of excimer based white OLEDs employ either bidentate or tridentate cyclometalating ligands, both of which have typically demonstrated external quantum efficiency (EQE) less than 20% and often poor CRI or Commission internationale de l'éclairage (CIE) coordinates.[16,17] One exception is the recent development of platinum(II) bis(methyl-imidazolyl)benzene chloride (Pt-16) resulted in a device with peak EQE of 20.1%, CRI of 80, and CIE of (0.33,0.33).[18] However, it was demonstrated that the monomer species of Pt-16 was inefficient, leading to a lower overall efficiency and an unavoidable tradeoff between optimal color and highest efficiency. Furthermore, the N^C^N complexes and other tridentate analogs require Cl^- or other monoanionic ligands as the fourth coordinating ligand which may be potentially unstable so a new molecular design motif is needed.[19] Here, we report the synthesis of a series of tetradentate Pt complexes based on a phenyl methyl-imidazole emissive ligand (**Figure 1**), which demonstrate efficient emission from both the excimer and monomer achieving a peak EQEs of 24% ± 2% for all three emitters at concentrations from 2% to 16%. The effect

T. Fleetham, L. Huang, Prof. J. Li
Material Science and Engineering
Arizona State University
Tempe, AZ 85284, USA
E-mail: Jian.li.1@asu.edu

DOI: 10.1002/adfm.201401244

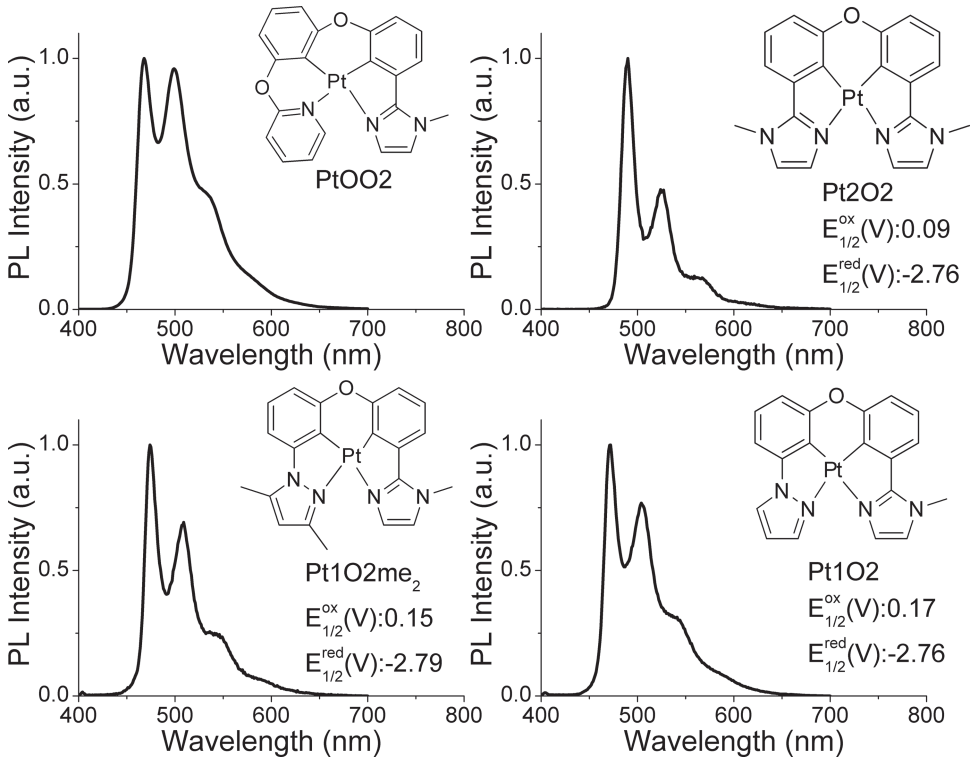

Figure 1. Photoluminescent emission spectra of PtOO2, Pt1O2, Pt2O2 and Pt1O2me$_2$ at room temperature in a solution of CH_2Cl_2 with the corresponding redox potentials inset.

of small structural changes to the ligand on the monomer and excimer emission properties were also studied with this class of emitters as well as the operational stability of an excimer emitting species. A device employing Pt2O2, in particular, achieved a device operational lifetime to 80% initial luminance estimated at over 200 h at 1000 cd m^{-2} while also achieving 12.5% peak EQE, CIE of (0.46,0.47), and a CRI of 80.

2. Results and Discussion

2.1. Efficient and Stable Monomer and Excimer Emission from Pt2O2

The previously reported blue emitter PtOO2 (Figure 1a) demonstrated a broad blue emission with emission onset just below 450 nm and a primary emission peak at 470 nm, which should serve well for stable and efficient white lighting due to its blue color and compatibility with the triplet energy of many stable host materials.[20] However, no excimer formation is observed for this complex due to the out of plane distortion of this class of tetradentate emitters. Recently, a symmetric tetradentate platinum complex, Pt7O7, employed a new design motif which improved the planarity for enhanced molecular stacking and demonstrated both efficient monomer and excimer emission.[21] Following the symmetric, planar backbone exhibited in Pt7O7, the complex Pt2O2 (Figure 1b) was synthesized. Despite retaining the same phenyl methyl-imidazole cyclometalating ligand as PtOO2, the primary emission peak of Pt2O2 was red shifted by 20 nm to 490 nm, which reduces the blue component of the emission spectrum, but such a molecule may still prove useful as an excimer based white OLED.

Devices of Pt2O2 were fabricated in the structure of ITO/HATCN(10 nm)/NPD(40 nm)/TAPC(10 nm)/*x*% Pt2O2:26mCPy(25 nm)/DPPS(10 nm)/BmPyPB(40 nm)/LiF/Al where HATCN is 1,4,5,8,9,11-hexaazatriphenylene-hexacarbonitrile, NPD is N,N′-diphyenyl-N,N′-bis(1-naphthyl)-1,1′-biphenyl-4,4″-diamine, TAPC is di-[4-(N,N-di-toylyl-amino)-phyenyl] cyclohexane, 26mCPy is 2,6-bis(N-carbazolyl) pyridine, DPPS is diphenyl-bis[4-(pyridin-3-yl)phenyl]silane, and BmPyPB is 1,3-bis[3, 5-di(pyridin-3-yl)phenyl]benzene.[22] For blue OLED devices with primarily monomeric emission character, the dopant concentration was controlled to be around 2% (w/w) to minimize the formation of excimers. The monochromatic devices demonstrated a very high peak EQE of 25.4% shown in **Figure 2** and **Table 1** and a peak power efficiency of 57.1 Lm/W. These efficiencies represent electron to photon conversion efficiencies approaching unity and are amongst the highest of any OLEDs without light outcoupling techniques. The electroluminescent spectrum, shown in the inset to Figure 2, demonstrated green emission with a primary peak at 496nm and CIE coordinates of (0.231, 0.565).

As the Pt2O2 dopant concentration is increased to 8%, 12%, and 16% the formation of a broad, red-shifted emission peak appears in the EL spectra (Figure 2 inset) which is attributed to the increased formation of excimers at the higher concentrations. This is in contrast to the observed concentration behavior of many other tetradentate platinum complexes such as PtOO2 and analogs.[20] This can be explained by the suspected planar nature of the Pt2O2 molecules compared to the

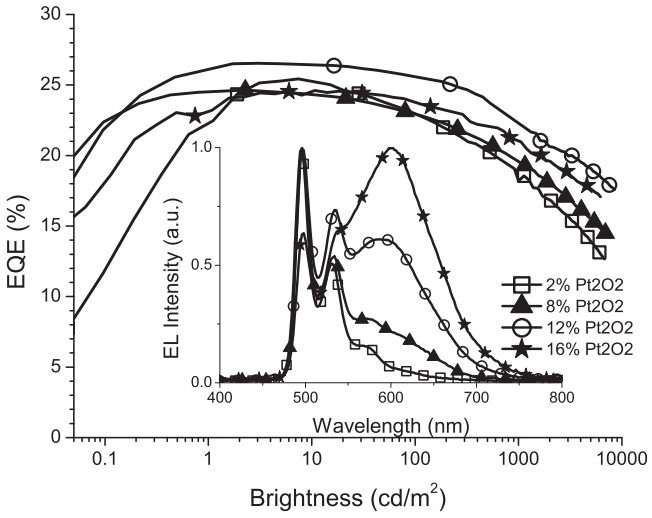

Figure 2. The EQE versus brightness plots for Pt2O2 devices in the structure: ITO/HATCN (10 nm)/NPD (40 nm)/TAPC (10 nm)/*x*% Pt2O2: 26mCPy (25 nm)/DPPS (10 nm)/BmPyPB (40 nm)/LiF (1 nm)/ Al for 2% (squares), 8% (triangles), 12% (circles), and 16% (stars). The corresponding EL spectra are inset.

twisted, non-planar geometry of PtOO2 shown in the previous report.[6a] Ultimately, an orange-white emission with CIE coordinates of (0.48,0.48) and CRI of 72 is achieved at a concentration of 16% Pt2O2. These moderate CRI values are achieved in spite of the lack of a portion of the blue emission spectrum due to the broad and balanced emission color across the rest of the visible range. Furthermore, it is very encouraging that both the monomer and excimer species are very efficient as evidenced by the very high peak EQE values at all concentrations with the highest achieved peak EQE value of 26.5% for 12% Pt2O2 doped devices and remaining as high as 24.6% for 16% doped devices. These high efficiencies are comparable or superior to the previously reported Pt7O7 emitter indicating that this design motif is both extremely efficient and color tunable through small structural modifications.[21] The high efficiency of this emitter is further supported by the photoluminescent quantum yields (PLQY) of 0.84 and 0.61 in thin films at dopant concentrations of 2% and 14%, respectively. Nevertheless, the PLQY may only provide part of the story because it is possible that a significant portion of excimers are generated directly from charge transfer between neighboring anion and cation species as opposed to going through an excited monomer intermediate.[15b] The existence of charge transfer generated excimers in these devices is evidenced by the large current density dependence in the emission spectrum (Supporting Information Figure S10) in contrast to many previous reports of excimer emitters. Uncovering the nature of excimer formation and the effect of molecular structure on the various formation mechanisms is a challenging and important task and is under continued study.

To further explore the effectiveness of excimer emitting platinum emitters, such as Pt2O2, as a commercially viable white light source, the device operational lifetime must also be evaluated. Unfortunately, many of the organic materials including the electron and hole blockers are known to dramatically reduce device stability due to electrochemical degradation.[23] In particular, the efficient device structure employing TAPC and DPPS layers is unsuitable for device operational lifetime testing, as demonstrated previously.[31] Consequently, a known stable, albeit inefficient, structure of ITO/HATCN (10 nm)/NPD (40 nm)/ 16% Pt2O2: CBP (25 nm)/BAlq (10 nm)/ Alq (30 nm)/ LiF/Al can be used, where CBP is 4,4′-bis(N-carbazolyl) biphenyl, BAlq is bis(2-methyl-8-quinolinolato)

Table 1. Performance parameters of devices in the structure: ITO/HATCN (10 nm)/NPD (40 nm)/TAPC (10 nm)/*x*% emitter:26mCPy (25 nm)/DPPS (10 nm)/BmPyPB(40)/LiF/Al.

				Peak			1000 cd/m^2		
Dopant	Conc. [% w/w]	CIE[a)]	CRI[a)]	η_{EQE}[b)] [%]	η_{PE}[b)] [Lm/W]	η_A[b)] [cd/A]	η_{EQE} [%]	η_{PE} [Lm/W]	η_A [cd/A]
Pt2O2	2	(0.231,0.565)	–	25.4	57.1	70.6	18.2	27.2	50.5
Pt2O2	8	(0.327,0.536)	42	24.6	58.5	66.6	19.6	28.2	52.9
Pt2O2	12	(0.411,0.512)	58	26.5	61.4	69.8	20.1	29.8	52.9
Pt2O2	14	(0.450,0.489)	68	24.1	50.9	59.6	21.4	29.9	52.8
Pt2O2	16	(0.475,0.478)	72	24.6	46.1	59.0	21.0	24.9	50.5
Pt1O2	2	(0.215,0.438)	–	24.1	47.6	55.8	16.9	20.0	38.9
Pt1O2	8	(0.359,0.455)	61	23.6	51.4	61.9	17.7	24.7	46.5
Pt1O2	12	(0.454,0.480)	61	23.1	53.5	64.7	18.5	27.5	51.6
Pt1O2	16	(0.485,0.479)	57	22.6	48.7	63.2	19.3	28.8	53.9
Pt1O2me$_2$	2	(0.229,0.440)	–	26.5	58.0	68.0	17.6	24.2	45.3
Pt1O2me$_2$	4	(0.318,0.496)	44	26.7	68.3	80.3	17.6	28.5	53.1
Pt1O2me$_2$	6	(0.354,0.513)	45	24.7	69.0	76.9	17.7	31.0	55.1
Pt1O2me$_2$	12	(0.416,0.528)	44	24.2	68.2	78.7	20.4	35.7	66.2
Pt1O2me$_2$	16	(0.422,0.531)	42	24.2	69.0	79.9	20.6	35.4	67.9

[a)]Color coordinates (CIE) and color rendering index (CRI) determined from spectrum collected at 1 mA/cm^2; [b)]η_{EQE} is the external quantum efficiency, η_{PE} is the power efficiency, and η_A is the current efficiency.

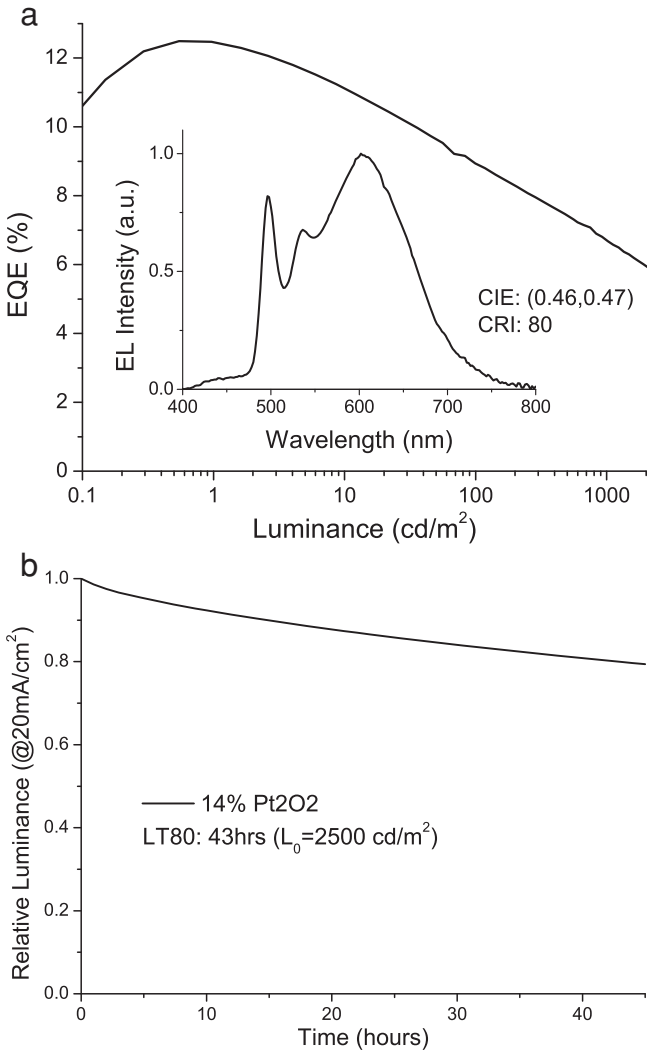

Figure 3. a) EQE vs. luminance and EL spectra at 1 mA/cm^2 (inset) and b) luminance versus time plots for Pt2O2 devices operated at a constant driving current of 20 mA/cm^2 with the initial luminance and T_{80} values are given in the inset to the plot. Devices are in the structure: ITO/HATCN (10 nm)/NPD (40 nm)/16% Pt2O2: CBP (25 nm)/BAlq (10 nm)/Alq (30 nm)/LiF (1 nm)/ Al.

(biphenyl-4-olato)aluminum and Alq is tris-(8-hydroxyquinoline) aluminum.[24] The resulting external quantum efficiency shown in **Figure 3**a is reduced to 12.5% due to the lack of state of the art blocking or transport materials resulting in charge imbalance or poor charge and exciton confinement. Furthermore, the large roll-off in the efficiency is attributed to the charge imbalance between the transport of the electrons and holes as the materials and device structure was selected to optimized stability rather than electrical properties. Nevertheless, such an efficiency is much higher that most previous reports employing a similar device structure.[21,24] The EL spectra (Figure 3a inset) shows similar emission to that observed in the efficient device structure except with the addition of a small peak between 400–500 nm indicating poor exciton confinement. Remarkably, this small deep blue peak complimented the warm white Pt2O2 color to yield a CRI of 80 and CIE of (0.46,0.47). Accelerated lifetime testing was preformed on the device by driving it at a constant current of 20 mA/cm^2 corresponding to an initial luminance of 2520 cd/m^2. The device demonstrated a lifetime to 80% of initial luminance (LT80) of 43 h at these elevated conditions. This corresponds to 207 h at 1000 cd/m^2 or over 10 000 h at 100 cd/m^2 using the conversion equation $LT(L_1) = LT(L_0)(L_0/L_1)^{1.7}$ where L_0 is the measured luminance and L_1 is the desired luminance.[25] Further application of state of the art stable host, charge and exciton blocker, and charge transport materials may yeild even greater lifetimes.[26] The acheivement of stable and efficient Pt2O2 doped white devices with peak EQE of 12.5%, CRI of 80 and LT80 of over 200 h at 1000 cd/m^2 is greater than that previously acheived for Pt7O7 and represents a significant step towards the possible commercializaiton of single doped OLEDs for solid state lighting.[21]

2.2. Tuning of Monomer and Excimer Emission

In order to achieve better CRI and CIE in a single doped white device it is necessary to blue shift the monomer emission of Pt2O2. By replacing one of the phenyl methylimidazole ligands of Pt2O2 with higher energy ligands of phenyl pyrazole (Pt1O2) or phenyl dimethylpyrazole (Pt1O2me$_2$), the PL emission (Figure 1) shifts to 474 nm and 472 nm respectively. In such a case, the triplet state is likely to be located on the lower energy phenyl methylimidazole ligand which acts as the lumophore. These values are in accordance with most reported Pt emitters containing phenyl methyl-imidazole emissive ligands and should serve well for achieving white light while remaining compatible with known stable carbazole-based host materials.[27] The redox potentials of the three emitters relative to a ferrocene/ferrocenium (Fc/Fc+) redox couple used as an internal reference, were determined using differential pulse voltammetry and are given in the inset to Figure 1. The data shows a lower oxidation potential for Pt2O2 compared with the asymmetric molecules indicating a shallower (higher energy) highest occupied molecular orbital (HOMO) energy level which reduces the bandgap in the case of Pt2O2. The origin for the red shift in Pt2O2 relative to its analogs is under continued investigation but is similar to the shift reported for other symmetric Pt complexes.[21,28]

Devices with various concentrations of Pt1O2 and Pt1O2me$_2$ where fabricated in the structure: ITO/HATCN(10 nm)/NPD(40 nm)/TAPC(10 nm)/*x*% emitter: 26mCPy(25 nm)/DPPS(10 nm)/BmPyPB(40 nm)/LiF/Al. As shown in **Figure 4** and Table 1, both Pt1O2 and Pt1O2me$_2$ are also very efficient across all tested concentrations. The peak external quantum efficiency ranged from 22.6% to 24.1% for Pt1O2 and 24.2% to 26.7% for Pt1O2me$_2$ while the power efficiency ranged from 47.6 to 53.5 Lm/W and 58.0 to 69.0 Lm/W respectively. These results further demonstrate the high efficiencies of both the monomer and excimer species characteristic for this class of emitters.

The emission spectra for white device of Pt2O2, Pt1O2, and Pt1O2me$_2$ are shown in **Figure 5** for concentrations of 14%, 12%, and 6%, respectively. In accordance with the difference in the PL spectra, the monomer emission peak of both Pt1O2 (480 nm) and Pt1O2me$_2$ (476 nm) is blue shifted relative to

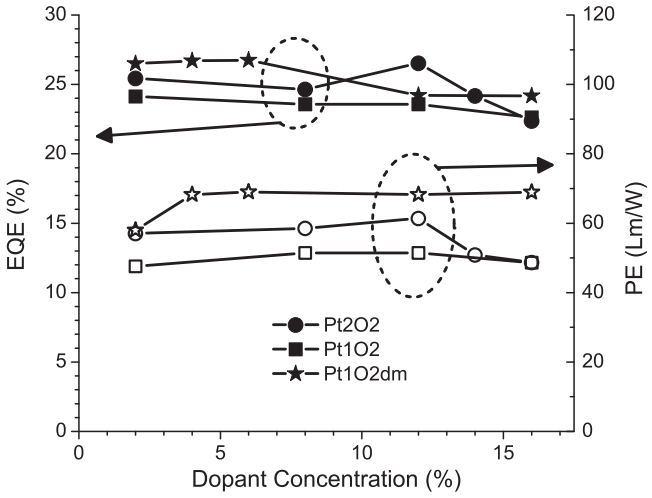

Figure 4. Peak EQE (solid symbols) and peak power efficiency (open symbols) for devices of Pt1O2, Pt2O2, and Pt1O2me$_2$ in the device structure: ITO/HATCN (10 nm)/NPD (40 nm)/TAPC (10 nm)/*x*% Dopant: 26 mCPy (25 nm)/DPPS (10 nm)/BmPyPB (40 nm)/LiF (1 nm)/Al.

Pt2O2 (496 nm). The excimer emission peak on the other hand, is only slightly blue shifted for Pt1O2 (592 nm) compared to Pt2O2 (600 nm) although it is more narrow. This similarity in excimer emission is as expected due to the similarity in shape and planarity of the two molecules.[29] The excimer emission of Pt1O2me$_2$, on the other hand, was significantly blue shifted to 556 nm. This shift may be related to distortion of the molecule due to the methyl group on the 5 position of the pyrazole which can modify the stacking orientation or increase the intermolecular spacing between the two dopant molecules. It is interesting however, that Pt1O2me$_2$ is capable of exhibiting such strong excimer character despite this potential geometric distortion, with nearly dominant excimer character at a Pt1O2me$_2$ concentration of only 8%. More synthetic and characterization efforts are needed to elucidate the relationship between the molecular structure, the excimer emission energy, and the concentration dependence. Thus, the choice of cyclometalating ligand needs to be carefully selected to control the influence on the energy of the monomer species as well as control the effect of steric groups on the geometry and stacking of the complexes.

An additional consequence of the efficient excimer emission at low concentrations for Pt1O2me$_2$ is the opportunity to explore the stability of the isolated excimer emissive species in a device setting. Device operational lifetime measurements were carried out for devices of the structure: ITO/HATCN (10 nm)/NPD (40 nm)/ 12% Pt1O2me$_2$:CBP (25 nm)/BAlq (10 nm)/Alq (30 nm)/LiF/Al. These devices exhibited nearly exclusive excimer emission which peaked at 567 nm yielding an orange color with CIE coordinates of (0.43, 0.50) as shown in **Figure 6**a. The devices were also moderately efficient with a peak EQE of 12.3%, which is similar to that achieved with Pt2O2 in the stable device structure. For operational lifetime testing, devices were driven at a constant current of 20 mA/cm^2, which corresponds to an initial luminance of 3060 cd/m^2. The device demonstrated an LT80 over 60 h, which corresponds to over 400 h at 1000 cd/m^2 and is among the highest for any Pt emitters. This long lifetime demonstrates that the excimer species can be very stable and should serve as a benchmark for future excimer based devices.

2.3. High Efficiency Multilayer White Devices

Due to the limited spectral coverage in the blue region, these Pt complexes can used as emitters in white devices employing multiple emissive layers to achieve a high efficiency and a high quality of white light. Due to the broad spectral coverage of the monomer and excimer emission, efficient OLEDs with emission covering most of the visible spectrum can be acheived using only two emissive materials. This is greatly desired compared to white OLEDs containing three or more emissive layers since the optimiztion of charge transport and energy transfer processes in white OLEDs becomes increasingly complex with additional layers.[30] Multilayer white OLEDs containing Pt2O2 and the previously reported deep blue emitter, PtON1, are fabricated in the structure ITO/HATCN(10 nm)/NPD(40 nm)/ TAPC(10 nm)/ 16% Pt2O2: 26mCPy (10 nm)/6% PtON1: 26mCPy/DPPS(10 nm)/BmPyPB(40 nm)/LiF/Al (15 nm).[31]

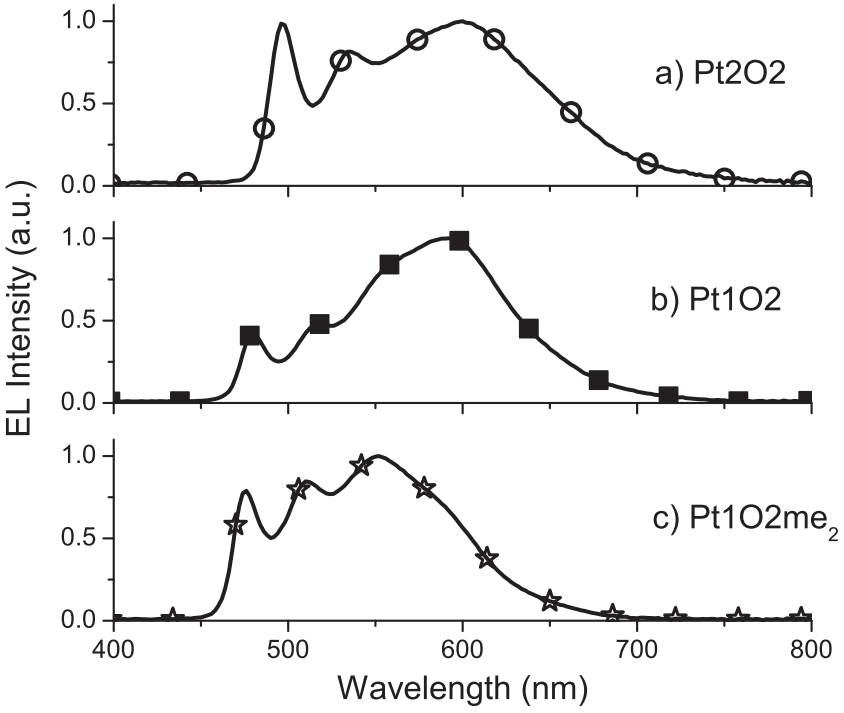

Figure 5. The EL spectra for white devices of a) 14% Pt2O2, b) 12% Pt1O2, and c) 6% Pt1O2me$_2$ in the structure: ITO/HATCN (10 nm)/NPD (40 nm)/TAPC (10 nm)/*x*% Dopant: 26mCPy (25 nm)/DPPS (10 nm)/BmPyPB (40 nm)/LiF (1 nm)/Al.

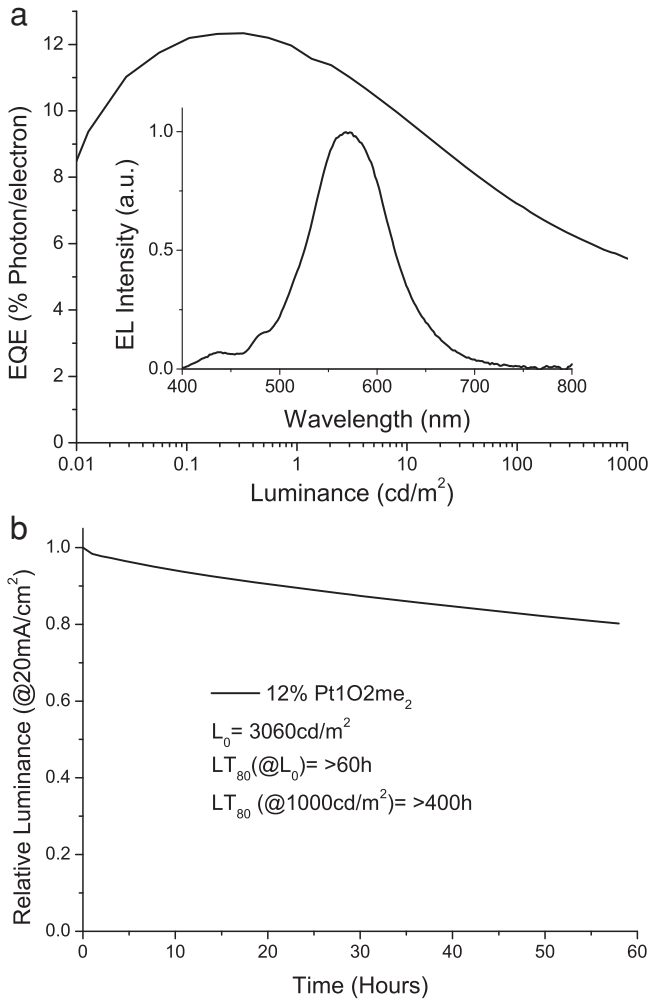

Figure 6. a) EQE vs. luminance and EL spectra at 1 mA/cm^2 (inset) and b) luminance versus time plots for Pt1O2me$_2$ operated at a constant driving current of 20 mA/cm^2 with the initial luminance and T_{80} values are given in the inset to the plot. Devices are in the structure: ITO/HATCN (10 nm)/NPD (40 nm)/ 12% Pt1O2me$_2$:CBP (25 nm)/BAlq (10 nm)/Alq (30 nm)/LiF (1 nm)/Al.

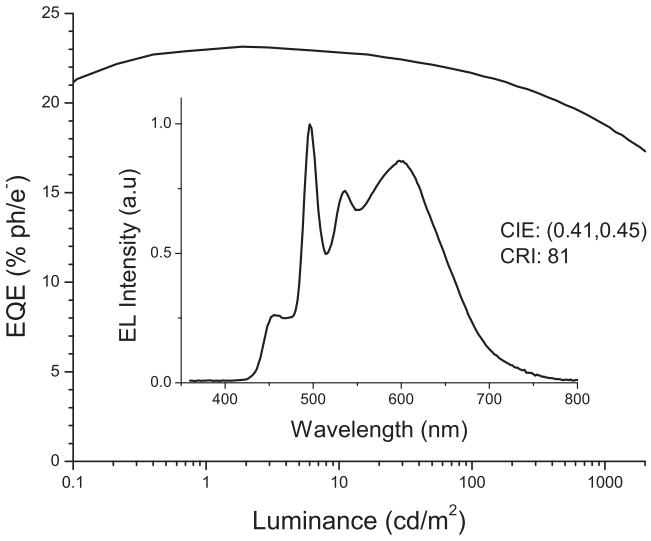

Figure 7. EQE vs. luminance and EL spectra at 1 mA/cm^2 (inset) for the multiple emissive layer white device in the structure: ITO/HATCN (10 nm)/NPD (40 nm)/TAPC (10 nm)/16% Pt2O2:26mCPy (10 nm)/6% PtON1:26mCPy (15 nm)/DPPS (10 nm)/BmPyPB(40)/LiF/Al.

The EQE, shown in **Figure 7**, peaked at 23.1% and the power efficiency peaked at 49.7 Lm/W. The device had low roll-off at high current densities remaining at 18.8% EQE and 24.2 Lm/W at 1000 cd/m^2. The emission spectrum showed a moderate deep blue contribution from PtON1 which dramatically improved the CRI to 81 and the CIE coordinates to (0.41,0.45). Further optimization and color balance of such devices is likely to yeild much greater performance but this demonstration underlines the importance of incoprorating the deep blue portion of the emission spectrum.

3. Conclusion

In summary, we have demonstrated a series of tetradentate Pt emitters that exhibited both efficient monomer and excimer emission. Through small modifications in the ancillary ligand both the monomer and excimer emission can be tuned. Furthermore, we demonstrated that the excimer species can be electrochemically stable in a device setting, achieving greater than 400 h at 1000 cd/m^2 for a device with emission nearly exclusively from the excimer species. A white OLED of Pt2O2 with an efficiency of 12.5%, CRI 80, and operational lifetime LT80 of over 200 h at 1000 cd/m^2 further illustrates the potential for this class of emitters to be a viable option for simple white OLEDs for solid state lighting. Further development of this class of emitters and ongoing work in the development of stable and efficient blocking, transport, and host materials will further speed the progress of this technology.

4. Experimental Section

General procedures: All commercial reagents were purchased and used as received without further purification. K_2PtCl_4 was purchased from Aldrich Chemical. $^nBu_4NBr$ and CuI were purchased from Aldrich Chemical. Silica gel (40–60μm) was purchased from Agela Technologies and BDH. The solvent, N,N-Dimethylacetamide (DMAc), was purchased from Sigma Aldrich.

^{1}H spectra were recorded at 400 MHz, ^{13}C NMR spectra were recorded at 100 MHz on Varian Liquid-State NMR instruments in DMSO-d_6 solutions. ^{1}H NMR spectra were recorded with residual solvent peak (δ = 2.50 ppm) as internal reference; ^{13}C NMR spectra were recorded with DMSO-d_6 (δ = 39.52 ppm) as internal reference. The following abbreviations (or combinations thereof) were used to explain ^{1}H NMR ultiplicities: s = singlet, d = doublet, t = triplet, m = multiplet. Mass spectra were recorded on a Voyager DE-STR MALDI-TOF mass spectrometer from Applied Biosystems. Photoluminescent emission spectra were performed on a Horiba Jobin Yvon FluoroLog-3 at room temperature and 77K in a solution of dichloromethane. The absolute PL quantum efficiency measurements of doped thin films were carried out on a Hamamatsu C9920 system equipped with a xenon lamp, integrating sphere and a model C10027 photonic multi-channel analyzer. The redox potentials are based on the values measured from differential pulsed voltammetry using a CHI610B electrochemical analyzer in a solution of anhydrous DMF (Aldrich) with 0.1 M tetra(n butyl)

ammonium hexafluorophosphate as the supporting electrolyte and are reported relative to a ferrocene/ferrocenium (Fc/Fc+) redox couple used as an internal reference. A silver wire was used as the pseudo reference electrode, a Pt wire was used as the counter electrode, and glassy carbon was used as the working electrode.

Synthesis of Pt2O2: To a 100 mL three-neck round bottom flask were added 1-methyl-2-(3-(3-(1-methyl-1*H*-imidazol-2-yl)phenoxy)phenyl)-1*H*-imidazole (165 mg, 0.5 mmol), potassium tetrachloroplatinate (218 mg, 0.52 mmol), and $^{n}Bu_4NBr$(16.1 mg, 0.05 mmol). The flask was evacuated and backfilled with nitrogen for three times and acetic acid (30 mL) was added under the protection of nitrogen. The reaction mixture was stirred at ambient temperature for 12 h and then followed at 120 °C for another 70 h under nitrogen atmosphere. After cooling to room temperature, the mixture was poured into 50 mL of water. The precipitate was collected through filtration, washed with water for three times and dried in air. The collected solid was purified by column chromatography on silica gel using dichloromethane as eluent to obtain a crude product, recrystallized in dichloromethane and ether to afford the desired platinum compound as a yellow solid (215 mg, 82%). ^{1}H NMR (DMSO-d_6, 400 MHz): δ 4.07 (s, 6H), 6.97 (d, J = 8.4 Hz, 2H), 7.14 (dd, J = 15.6, 8.0 Hz, 2H), 7.37 (d,, J = 7.2 Hz, 2H), 7.45 (s, 2H), 7.53 (d, J = 1.2 Hz, 2H).). ^{13}C NMR (DMSO-d_6, 100 MHz): δ 35.15, 116.30, 117.25, 123.20, 126.70, 123.58, 138.19, 150.98, 155.70. MS (MALDI) for $C_{20}H_{16}N_4OPt$ $[M]^+$: calcd 524.1, found 524.2.

Synthesis of Pt1O2me$_2$: To a 100 mL three-neck round bottom flask were added 3,5-dimethyl-1-(3-(3-(1-methyl-1*H*-imidazol-2-yl)phenoxy)phenyl)-1*H*-pyrazole (172 mg, 0.5 mmol), potassium tetrachloroplatinate (218 mg, 0.52 mmol) and $^{n}Bu_4NBr$(16.1 mg, 0.05 mmol). The flask was evacuated and backfilled with nitrogen for three times and acetic acid (30 mL) was added under the protection of nitrogen. The reaction mixture was stirred at ambient temperature for 12 h and then followed at 120 °C for another 70 h under nitrogen atmosphere. After cooling to room temperature, the mixture was poured into 50 mL of water. The precipitate was collected through filtration, washed with water for three times and dried in air. The collected solid was purified by column chromatography on silica gel using dichloromethane as eluent to obtain a crude product, recrystallized in dichloromethane and ether to afford the desired platinum compound as a yellow solid (205 mg, 77%). ^{1}H NMR (DMSO-d_6, 400 MHz): δ): δ 2.67 (s, 3H), 2.74 (s, 3H), 4.10 (s, 3H), 6.43 (s, 1H), 6.90 (d, J = 7.6 Hz, 1H), 7.01 (d, J = , 8.0, 1H), 7.14–7.23 (m, 2H), 7.26 (d, J = 8 Hz, 1H), 7.44–7.50 (m, 3H). ^{13}C NMR (DMSO-d_6, 100 MHz): δ 14.44, 14.81, 35.61, 106.66, 110.01, 112.73, 113.06, 116.37, 117.32, 123.48, 123.81, 123.89, 123.94, 128.51, 137.89, 141.34, 147.21, 150.25, 150.51, 151.46, 155.58. MS (MALDI) for $C_{21}H_{18}N_4OPt$ $[M]^+$: calcd 537.1, found 537.4.

Synthesis of Pt1O2: To a 100 mL three-neck round bottom flask were added added 1-(3-(3-(1-methyl-1*H*-imidazol-2-yl)phenoxy)phenyl)-1*H*-pyrazole (380 mg, 1.2 mmol), potassium tetrachloroplatinate (524 mg, 1.26 mmol) and $^{n}Bu_4NBr$ (38 mg, 0.12 mmol). The flask was evacuated and backfilled with nitrogen for three times and acetic acid (60 mL) was added under the protection of nitrogen. The reaction mixture was stirred at ambient temperature for 12 h and then followed at 120 °C for another 70 h under nitrogen atmosphere. After cooling to room temperature, the mixture was poured into 100 mL of water. The precipitate was collected through filtration, washed with water for three times and dried in air. The collected solid purified by column chromatography on silica gel using dichloromethane as eluent to obtain a crude product, recrystallized in dichloromethane and ether to afford the desired platinum compound as a yellow solid 220 mg, 36%). ^{1}H NMR (DMSO-d_6, 400 MHz): δ 4.08 (s, 3H), 6.80 (dd, J = 6.5, 2 Hz, 1H), 6.91 (d, J = 7.6 Hz, 1H), 7.01 (d, J = 8.4 Hz, 1H), 7.14–7.20 (m, 2H), 7.41 (d, J = 8.0 Hz, 2H), 7.48 (d, J = 1.2 Hz, 1H),), 7.65 (d, J = 1.2 Hz, 1H),), 8.38 (d, J = 1.6 Hz, 1H), 8.79 (d, J = 3.5 Hz, 1H). ^{13}C NMR (DMSO-d_6, 100 MHz): δ 35.19, 105.88, 107.78, 113.16, 116.01, 116.59, 117.54, 123.71, 123.81, 123.92, 124.51, 126.81, 128.30, 138.12, 141.37, 146.09, 150.98, 151.71, 155.35. MS (MALDI) for $C_{19}H_{14}N_4OPt$ $[M]^+$: calcd 509.1, found 509.3.

Device Fabrication and Characterization: Devices were fabricated on glass substrates pre-coated with a patterned transparent indium tin oxide (ITO) anode in the structure of ITO/HATCN(10 nm)/NPD(40 nm)/TAPC(10 nm)/*x*% dopant: 26mCPy(25 nm)/DPPS(10 nm)/BmPyPB(40 nm)/LiF/Al where HATCN is 1,4,5,8,9,11-hexaazatriphenylene-hexacarbonitrile, NPD is N,N′-diphyenyl-N,N′-bis(1-naphthyl)-1,1′-biphenyl-4,4″-diamine, TAPC is di-[4-(N,N-di-toylyl-amino)-phyenyl]cyclohexane, 26 mCPy is 2,6-bis(N-carbazolyl)pyridine, DPPS is diphenyl-bis[4-(pyridin-3-yl) phenyl]silane, and BmPyPB is 1,3-bis[3, 5-di(pyridin-3-yl)phenyl]benzene. For the stability devices the following structure was used: ITO/HATCN (10 nm)/NPD (40 nm)/x% dopant: CBP (25 nm)/ BAlq (10 nm)/Alq (30 nm)/LiF/Al where CBP is 4,4′-bis(N-carbazolyl) biphenyl, BAlq is bis(2-methyl-8-quinolinolato) (biphenyl-4-olato)aluminum, and Alq is tris-(8-hydroxyquinoline) aluminum. All small molecular materials were sublimed in a thermal gradient furnace prior to use. Prior to organic depositions, the ITO substrates were cleaned by sonication in water, acetone, and isopropanol followed by UV-ozone treatment for 15 minutes. Organic materials were thermally evaporated at deposition rates of .5 to 1.5 Å/s monitored by quartz crystal microbalances at a working pressure of less than 10^{-7} Torr. Aluminum deposited at a rate of 1–2 Å/s through a shadow mask without breaking vacuum defining a device areas of 0.04 cm^2 in a crossbar structure. All device operation and measurement were done inside a nitrogen-filled glove-box. I-V-L characteristics were taken with a Keithley 2400 Source-Meter and a Newport 818 Si photodiode. EL spectra were taken using an Ocean Optics HR4000 spectrometer. Agreement between luminance, optical power and EL spectra was verified with a calibrated Photo Research PR-670 Spectroradiometer with all devices assumed to be Lambertian emitters.

Supporting Information

Supporting Information is available from the Wiley Online Library or from the author.

Acknowledgements

The authors thank the National Science Foundation (CHE-0748867), Department of Energy (contract no. EE0005075), Universal Display Corporation, and Advanced Photovoltaics Center for partial support of this work. The authors also want to thank Dr. Jason Brooks from Universal Display Corporation for the measurement of absolute emission quantum yields of samples in thin film.

Received: April 18, 2014
Revised: May 25, 2014
Published online: July 24, 2014

[1] a) J. Kalinowski, V. Fattori, M. Cocchi, J. A. G. Williams, *Coord. Chem. Rev.* **2011**, *255*, 2401; b) L. Xiao, Z. Chen, B. Qu, J. Luo, S. Kong, Q. Gong, J. Kido, *Adv. Mater.* **2011**, *23*, 926.

[2] a) R. H. Friend, R. W. Gymer, A. B. Holmes, J. H. Burroughes, R. N. Marks, C. Taliani, D. D. C. Bradley, D. A. Dos Santos, J. L. Brédas, M. Lögdlund, W. R. Salaneck, *Nature* **1999**, *397*, 121; b) X. Yang, D. C. Müller, D. Neher, K. Meerholz, *Adv. Mater.* **2006**, *18*, 948; c) P. T. Furuta, L. Deng, S. Garon, M. E. Thompson, J. M. J. Frechét, *J. Am. Chem. Soc.* **2004**, *126*, 15388; d) P. R. Christensen, J. K. Nagle, A. Bhatti, M. O. Wolf, *J. Am. Chem. Soc.* **2013**, *135*, 8109; e) J. R. Sommer, R. T. Farley, K. R. Graham, Y. Yang, J. R. Reynolds, J. Xue, K. Schanze, *ACS Appl. Mater. Interfaces* **2009**, *1*, 274.

[3] a) S. Lee, S.-O. Kim, H. Shin, H.-J. Yun, K. Yang, S.-K. Kwon, J.-J. Kim, Y.-H. Kim, *J. Am. Chem. Soc.* **2013**, *135*, 14321; b) C.-H. Lin, Y.-Y. Chang, J.-Y. Huang, C.-Y. Lin, Y. Chi, M.-W. Chung,

C.-L. Lin, P.-T. Chou, G.-H. Lee, C.-H. Chang, W.-C. Lin, *Angew. Chem. Int. Ed.* **2011**, *50*, 3182; c) S.-C. Lo, R. E. Harding, C. P. Shipley, S. G. Stevenson, P. L. Burn, I. D. W. Samuel, *J. Am. Chem. Soc.* **2009**, *131*, 16681; d) T. Qin, J. Ding, L. Wang, M. Baumgarten, G. Zhou, K. Müllen, *J. Am. Chem. Soc.* **2009**, *131*, 14329; e) C.-H. yang, Y.-M. Cheng, Y. Chi, C.-J. Hsu, F.-C Fang, K.-T. Wong, P.-T. Chou, C.-H. Chang, M.-H. Tsai, C.-C. Wu, *Angew. Chem. Int. Ed.* **2008**, *47*, 4542; f) N. R. Evans, L. S. Devi, C. S. K. Mak, S. E. Watkins, S. I. Pascu, A. Köhler, R. H. Friend, C. K. Williams, A. B. Holmes, *J. Am. Chem. Soc.* **2006**, *128*, 6647; g) X. Yang, D. C. Müller, D. Neher, K. Meerholz, *Adv. Mater.* **2006**, *18*, 948; h) Y. You, S. Y. Park, *J. Am. Chem. Soc.* **2005**, *127*, 12438; i) Md. K. Nazeeruddin, R. Humphry-Baker, D. Berner, S. Rivier, L. Zuppiroli, M. Graetzel*J. Am. Chem. Soc.* **2003**, *125*, 8790.

[4] a) Z. M. Hudson, C. Sun, M. G. Helander, Y.-L. Chang, Z.-H. Lu, S. Wang, *J. Am. Chem. Soc.* **2012**, *134*, 13930; b) J. Kalinowski, V. Fattori, M. Cocchi, J. A. G. Williams, *Coord. Chem. Rev.* **2011**, *255*, 2401; c) M.-Y. Yuen, S. C. F. Kui, K.-H. Low, C.-C. Kwok, S. S.-Y. Chui, C.-W. Ma, N. Zhu, C.-M. Che, *Chem. Eur. J.* **2010**, *16*, 14131; d) L. Zhao, K. M.-C. Wong, B. Li, W. Li, N. Zhu, L. Wu, V. W.-W. Yam, *Chem. Eur. J.* **2010**, *16*, 6797; e) C. Che, C. Kwok, S. Lai, A. Rausch, W. Finkenzeller, N. Zhu, H. Yersin, *Chem. Eur. J.* **2010**, *16*, 233; f) V. N. Kozhevnikov, B. Donnio, D. W. Bruce, *Angew. Chem. Int. Ed.* **2008**, *47*, 6286; g) J. Kavitha, S.-Y. Chang, Y. Chi, J.-K. Yu, Y.-H. Hu, P.-T. Chou, S.-M. Peng, G.-H. Lee, Y.-T. Tao, C.-H. Chien, A. J. Carty, *Adv. Funct. Mater.* **2005**, *15*, 223; h) P. T. Furuta, L. Deng, S. Garon, M. E. Thompson, J. M. J. Frechét, *J. Am. Chem. Soc.* **2004**, *126*, 15388; i) X. Yang, Z. Wang, S. Madakuni, J. Li, G. E. Jabbour, *Adv. Mater.* **2008**, *20*, 2405.

[5] a) M. A. Baldo, D. F. O'Brien, Y. You, A. Shoustikov, S. Sibley, M. E. Thompson, S. R. Forrest, *Nature* **1998**, *395*, 151; b) M. A. Baldo, S. Lamansky, P. E. burrows, M. E. Thompson, S. R. Forrest, *Appl. Phys. Lett.* **1999**, *75*, 4; c) C. Adachi, M. A. Baldo, M. E. Thompson, S. R. Forrest, *J. Appl. Phys.* **2001**, *90*, 5048.

[6] a) E. Turner, N. Bakken, J. Li, *Inorg. Chem.* **2013**, *52*, 7344; b) S. C. F. Kui, P. K. Chow, G. Cheng, C-C. Kwok, C. L. Kwong, K.-H. Low, C.-M. Che, *Chem. Commun.* **2013**, *49*, 1497.

[7] a) M. C. Gather, A. Kohnen, K. Meerholz, *Adv. Mater.* **2011**, *23*, 233; b) K. T. Kamtekar, A. P. Monkman, M. R. Bryce, *Adv. Mater.* **2010**, *22*, 572.

[8] F. So, J. Kido, P. Burrows, *MRS Bull.* **2008**, *33*, 663.

[9] a) B. W. D'Andrade, R. J. Holmes, S. R. Forrest, *Adv. Mater.* **2004**, *16*, 624; b) J.-H. Jou, S.-M. Shen, C.-R. Lin, Y.-S. Wang, Y.-C. Chou, S.-Z. Chen, Y.-C. Jou, *Org. Electron.* **2011**, *12*, 865.

[10] a) R. S. Deshpande, V. Bulovic, S. R. Forrest, *Appl. Phys. Lett.* **1999**, *75*, 888; b) X. Gong, S. Wang, D. Moses, G. C. Bazan, A. J. Heeger, *Adv. Mater.* **2005**, *17*, 2053; c) Y. Zhao, J. Chen, D. Ma, *Appl. Phys. Lett.* **2011**, *99*, 163303; d) Y.-S. Park, J.-W. Kang, D. M. Kang, J.-W. Park, Y.-H. Kim, S.-K. Kwon, J.-J. Kim, *Adv. Mater.* **2008**, *20*, 1957; e) H. Sasabe, J. Takamatsu, T. Motoyama, S. Watanabe, G. Wagenblast, N. Langer, O. Molt, E. Fuchs, C. Lennartz, J. Kido, *Adv. Mater.* **2010**, *22*, 5003.

[11] a) Y. Sun, N. C. Giebink, H. Kanno, B. Ma, M. E. Thompson, S. R. Forrest, *Nature* **2006**, *440*, 908; b) B.-P. Yan, C. C. C. Cheung, S. C. F. Kui, H.-F. Xiang, V. A. L. Roy, S.-J. Xu, C.-M. Che, *Adv. Mater.* **2007**, *19*, 3599; c) G. Schwartz, M. Pfeiffer, S. Reineke, K. Walzer, K. Leo, *Adv. Mater.* **2007**, *19*, 3672; d) G. Schwartz, S. Reineke, T. C. Rosenow, K. Walzer, K. Leo, *Adv. Funct. Mater.* **2009**, *19*, 1319.

[12] S. Reineke, F. Lindner, G. Schwartz, N. Seidler, K. Walzer, B. Lüssem, K. Leo, *Nature* **2009**, *459*, 234.

[13] B. W. D'Andrade, M. E. Thompson, S. R. Forrest, *Adv. Mater.* **2002**, *14*, 147.

[14] B. W. D'Andrade, S. R. Forrest, *Adv. Mater.* **2004**, *16*, 1585.

[15] a) V. Adamovich, J. Brooks, A. Tamayo, A. M. Alexander, P. I. Djurovich, B. W. D'Andrade, C. Adachi, S. R. Forrest, M. E. Thompson, *New J. Chem.* **2002**, *26*, 1171; b) J. Kalinowski, M. Cocchi, L. Murphy, J. A. G. Williams, V. Fattori, *Chem. Phys.* **2010**, *378*, 47; c) S. C. F. Kui, P. K. Chow, G. S. M. Tong, S.-L. Lai, G. Cheng, C.-C. Kwok, K.-H. Low, M. Y. Ko, C.-M. Che, *Chem Eur. J.* **2013**, *19*, 69.

[16] E. L. Williams, K. Haavisto, J. Li, G. E. Jabbour, *Adv. Mater.* **2007**, *19*, 197.

[17] a) X. Yang, Z. Wang, S. Madakuni, J. Li, G. E. Jabbour, *Adv. Mater.* **2008**, *20*, 2405; b) N. Bakken, Z. Wang, J. Li, *J. Photon. Energy* **2012**, *2*, 021203.

[18] a) T. Fleetham, Z. Wang, J. Li, *Org. Electon.* **2012**, *13*, 1430; b) T. Fleetham, J. Ecton, Z. Wang, N. Bakken, J. Li, *Adv. Mater.* **2013**, *25*, 2573.

[19] a) N. C. Giebink, B. W. DAndrade, M. S. Weaver, P. B. Mackenzie, J. J. Brown, M. E. Thompson, S. R. Forrest, *J. Appl. Phys.* **2008**, *103*, 044501; b) V. Sivasubramaniam, F. Brodkorb, S. Hanning, H. P. Loebl, V. Elsbergen, H. Boerner, U. Scherf, M. Kreyenschmidt, *J. Fluorine Chem.* **2009**, *130*, 640.

[20] J. Ecton, T. Fleetham, X. Hang, J. Li, *SID Int. Symp. Dig. Tech.* **2013**, *44*, 152.

[21] G. Li, T. Fleetham, J. Li, *Adv. Mater.* **2014**, *26*, 2931.

[22] a) L. Xiao, S-J. Su, Y. Agata, H. Lan, J. Kido, *Adv. Mater.* **2009**, *21*, 1271; b) H. Sasabe, E. Gonmori, T. Chiba, Y. J. Li, D. Tanaka, S.-J. Su, T. Takeda, Y-J. Pu, K. Nakayama, J. Kido, *Chem. Mater.* **2008**, *20*, 5951; c) N. Chopra, J. S. Swensen, E. Polikarpov, L. Cosimbescu, F. So, A. B. Padmaperuma, *Appl. Phys. Lett.* **2010**, *97*, 033304.

[23] M. Segal, C. Mulder, K. Celebi, M. Singh, K. Rivoire, S. Difley, T. Van Voorhis, M. A. Baldo, *Proc. SPIE, 6999* **2008**, 699912.

[24] R. C. Kwong, M. R. Nugent, L. Michalski, T. Ngo, K. Rajan, Y-J. Tung, M. S. Weaver, T. X. Zhou, M. Hack, M. E. Thompson, S. R. Forrest, J. J. Brown, *Appl. Phys. Lett.* **2002**, *81*, 162.

[25] C. Féry, B. Racine, D. Vaufrey, H. Doyeux, S. Cinà, *Appl. Phys. Lett.* **2005**, *87*, 213502.

[26] a) H. Fukagawa, T. Shimizu, H. Hanashima, Y. Osada, M. Suzuki, H. Fujikake, *Adv. Mater.* **2012**, *24*, 5099; b) H. Nakanotani, K. Masui, J. Nishide, T. Shibata, C. Adachi, *Sci. Rep.* **2013**, *3*, 2127.

[27] X. Ren, J. Li, R. J. Holmes, P. I. Djurovich, S. R. Forrest, M. E. Thompson, *Chem. Mater.* **2004**, *16*, 4743.

[28] D. A. K. Vezzu, J. C. Deaton, J. S. Jones, L. Bartolotti, C. F. Harris, A. P. Marchetti, M. Kondakova, R. D. Pike, S. Huo, *Inorg. Chem.* **2010**, *49*, 5107.

[29] B. Ma, J. Li, P. I. Djurovich, M. Yousufuddin, R. Bau, M. E. Thompson, *J. Am. Chem. Soc.* **2005**, *127*, 28.

[30] R. Wang, D. Liu, H. Ren, T. Zhang, H. Yin, G. Liu, J. Li, *Adv. Mater.* **2011**, *23*, 2823.

[31] X. Hang, T. Fleetham, E. Turner, J. Brooks, J. Li, *Angew. Chem. Int. Ed.* **2013**, *52*, 6753.